

## Research Article

# Explosion Pressure and Minimum Explosible Concentration Properties of Metal Sulfide Ore Dust Clouds

Yun-zhang Rao,<sup>1</sup> Chang-shun Tian ,<sup>1</sup> Wei Xu,<sup>1</sup> Chun-yu Xiao,<sup>1</sup> Bo-yun Yuan,<sup>2</sup> and Yao Yu<sup>1</sup>

<sup>1</sup>Faculty of Resources and Environmental Engineering, Jiangxi University of Science and Technology, Ganzhou 341000, China

<sup>2</sup>Jiangle County Natural Resources Bureau, Jiangle 353300, China

Correspondence should be addressed to Chang-shun Tian; 15581044@qq.com

Received 18 September 2019; Revised 14 December 2019; Accepted 6 January 2020; Published 30 January 2020

Academic Editor: Hakan Arslan

Copyright © 2020 Yun-zhang Rao et al. This is an open access article distributed under the Creative Commons Attribution License, which permits unrestricted use, distribution, and reproduction in any medium, provided the original work is properly cited.

The explosion pressure and minimum explosible concentration (MEC) properties of metal sulfide ore dust clouds are valuable for the prevention and control of metal sulfide ore dust explosions. In this study, a 20 L explosion sphere vessel was used to investigate the effect of sulfur content, particle size, and concentration on the explosion pressure and minimum explosible concentration of metal sulfide ore dust clouds. Four samples with different sulfur contents were selected (30%–40%, 20%–30%, 10%–20%, and 0%–10%). Before and after the explosion, samples were tested by X-ray diffraction. The results indicate that the metal sulfide ore dust is explosive dust with St1 grade explosion pressure. With an increase in concentration, the maximum explosion pressure increased at first and then decreased. With an increase in sulfide content, the explosion pressure of metal sulfide ore dust increased, while the minimum explosible concentration decreased. As particle size decreased, the MEC also decreased. The sulfur content, particle size, and concentration of metal sulfide ore dust were the main factors affecting the explosion hazard.

## 1. Introduction

Metal sulfide ores are widely applied in industrial production of products, such as jewelry, automobile parts, and electronic equipment. The most common metal sulfide ores are pyrite. In addition, sulfide ores include chalcopyrite (copper ore), molybdenite (molybdenum ore), sphalerite (zinc ore), galena (lead ore), and cinnabar (mercury ore) [1]. Because of the chemical activity of sulfur and iron and the variable valence [2], they can readily undergo spontaneous combustion and even explosion. Furthermore, a lot of sulfide dust is dispersed into the air to form dispersed gas-solid mixtures, and satisfactory conditions can lead to a significant explosion risk [3–6]. In recent years, an increased frequency in metal sulfide ore dust explosion accidents has resulted in injuries and losses to life and property in Europe, Canada, South Africa, Australia, the former Soviet Union, China, and other countries, as displayed in Table 1 [7, 8]. However, studies on the dust explosion of metal sulfide ores are limited. Therefore, studying explosion characteristics of metal sulfide ore dust is important for preventing and controlling major hazardous accidents in various industries.

The explosion characteristic parameters of dust mainly include the maximum explosion pressure ( $P_{max}$ ), minimum explosible concentration (MEC), maximum explosion pressure rise rate ( $(dP/dt)_{max}$ ), and explosion index ( $K_{st}$ ). Among them,  $P_{max}$ ,  $(dP/dt)_{max}$ , and  $K_{st}$  are used to characterize the severity of dust explosion consequences, whereas the MEC is used to characterize the possibility of dust explosions [9]. Many studies have experimentally considered the explosion parameters of dust and factors influencing dust explosion parameters.

**1.1. Effect of Particle Size.** A sulfide dust explosion is less severe than the explosion of carbonaceous dusts, such as cornstarch and wheat flour. Compared with other combustible dusts in underground mines, sulfide dust is also less hazardous than bituminous coal dust and higher-grade oil shale dust [10]. Pyrite has been found to be more explosible than pyrrhotite, and fine particles make a significant contribution to explosibility [8]. The risk and strength of the explosion of sulfur dust decrease with increasing particle size [11]. With a decrease in particle size, the measured MEC

TABLE 1: Reported cases of sulfide dust explosions.

| Date      | Country | Fatalities | Injuries |
|-----------|---------|------------|----------|
| 1924      | USA     | 4          | 8        |
| 1926      | USA     | 3          | 1        |
| 1960s     | Canada  | 2          | 0        |
| 1969      | Sweden  | 2          | 2        |
| 1970~1974 | China   | 5          | 10       |
| 1978      | China   | 4          | 0        |
| 1979      | China   | 4          | 0        |
| 1985      | Canada  | 1          | 2        |
| 2002      | China   | 2          | 0        |
| 2004      | China   | 3          | 0        |

becomes lower, and the measured MEC has an approximate linear relation with particle size [12]. The influence of dust particle size on  $P_{\max}$  and  $(dP/dt)_{\max}$  is relatively small because of the condensation between the heated volume expansion of sulfur particles and sulfur droplets [13]. At the same dust concentration,  $P_{\max}$  and  $K_{st}$  all increase with decreasing particle size [14]. Irregularly shaped dust has a lower MIE compared to spherical-shaped dust because of the higher specific surface area of irregularly shaped dust, which affects dust cloud dynamics and leads to a lower resistance to thermal conduction [15]. For selected nanopowders, there does not seem to be an explosion difference between different particle sizes because the characteristic diameters are mainly affected by agglomeration; however, for microsized aluminum powders, the explosion characteristics decrease with an increase in particle size [16–18].

**1.2. Effect of Sulfur Content.** When the sulfur content of the sulfide dust cloud increases, more sulfur gas is produced by heating during ignition, heat is more sufficiently released from sulfur combustion, and the MIE required for ignition and explosion of sulfide dust is reduced [19, 20].

**1.3. Effect of Concentration.**  $P_{\max}$  and  $K_{st}$  increase at first and then decrease with increasing mass concentration [21, 22]. For  $P_{\max}$  and  $(dP/dt)_{\max}$  of sulfur dust, the effect of dust mass concentration is stronger than that of ignition energy, and the effect of ignition energy is stronger than that of particle size [11]. The effect of rubber dust mass concentration on  $P_{\max}$  and  $K_{st}$  is obvious.  $P_{\max}$  and  $K_{st}$  increase at first and then decrease with increasing mass concentration [23].

The explosion of sulfide dust is a complex unsteady gas-solid two-phase dynamic process [23]. Therefore, it is important to study the explosion parameters of metal sulfide ore dust during explosion to guide the prevention and control of mine disasters caused by dust explosions. In this study, four metal sulfide ore dusts were investigated using a 20 L explosion sphere vessel to examine the  $P_{\max}$  and MEC of metal sulfide ore dust clouds and factors influencing dust explosion parameters. Comprehensive experimental data and phenomenon analysis of the explosion of sulfide mine dust clouds are provided, and the mechanisms influencing sulfide mine dust cloud explosions are revealed based on existing theories.

## 2. Materials and Experimental Methods

**2.1. Materials and Characterization.** Metal sulfide ores (pyrite,  $\text{FeS}_2$ ) were obtained from Dongxiang Copper Mine, Jiangxi Province, China, mainly because many accidents of sulfide ore dust combustion and explosion have been reported in the mine [24]. To ensure accuracy of sampling, multiple times and multipoint sampling methods were adopted. To prevent or reduce oxidation during transportation, a polyethylene film was used to wrap the sulfide ores, as shown in Figure 1. The sulfur content of the ores was determined by the combustion neutralization method and was as per the GB/T 2462-1996 standard [25]. The samples were burnt in an air flow at  $850^\circ\text{C}$ , and the sulfur in the sulfur monomer and sulfide was converted into sulfur dioxide gas and absorbed and oxidized into sulfuric acid using a hydrogen peroxide solution. Methyl red-methylene blue was used as an indicator, and sodium hydroxide standard titration solution was used for titration. The samples were divided into ultra-high sulfur ores A (sulfur content 30–40%), high sulfur ores B (sulfur content 20–30%), medium sulfur ores C (sulfur content 10–20%), and low sulfur ores D (sulfur content 0–10%).

The ores were crushed in the laboratory. To reduce oxidation of the surfaces during crushing, the ores were not scrapped too finely (Figure 2). The crushed ores were screened through sieves with pore sizes of 10 mm and 1.25 mm. To avoid the influence of water content on grinding, the crushed ore samples were dried at  $40^\circ\text{C}$  for 24 h. An XZM-100 grinder (Wuhan Prospecting Machinery Factory, China) was used to finely crush the ores. The ores were crushed through 200 mesh ( $75\ \mu\text{m}$ ), 300 mesh ( $48\ \mu\text{m}$ ), and 500 mesh ( $25\ \mu\text{m}$ ) sieves (Jiufeng Sieve, China; implementing Standards of GB/T 6003.1-2012 [26]). The samples were numbered A200, A300, A500, B200, B300, B500, C200, C300, C500, D200, D300, and D500. They were collected and put into polyvinyl chloride bags for further analysis.

The particle sizes of the four samples (A, B, C, and D) were tested using a Winner 2000 laser particle size analyzer. The results are shown in Figure 3. D50 (the particle size, whose cumulative distribution of particles is 50%) was used as the average particle size of the sample, supplemented by the analysis of the proportion of the main particle size range in each group of samples. As we can see from Figure 3, the proportion of particle sizes less than  $10\ \mu\text{m}$  is the largest as it exceeds 50%. The mineral dust of the particle size can be stably suspended in air to form stable dust clouds.

The main mineral components of the four samples were identified by Empyrean X-ray diffraction (XRD), and the results are shown in Figure 4. According to the identification results, a quantitative test and analysis of S, Fe, Si, and other elements were carried out; the analysis results are shown in Table 2. It can be seen from Figure 4 and Table 2 that all the four ore samples contain pyrite ( $\text{FeS}_2$ ) and silica ( $\text{SiO}_2$ ). Among them, pyrite ( $\text{FeS}_2$ ) is the main component leading to fire and explosion in vulcanized mines [27].

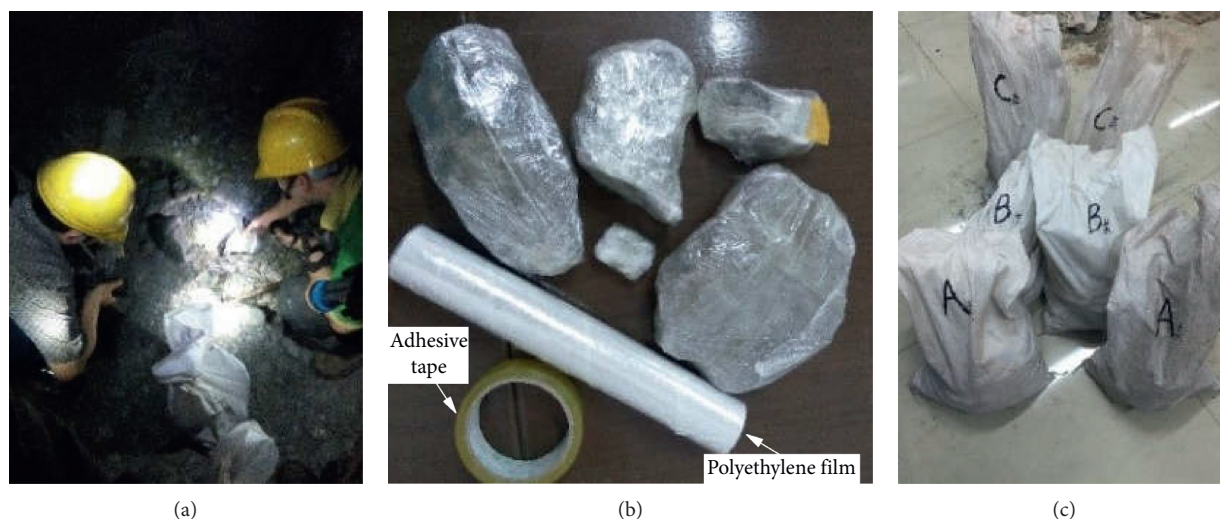


FIGURE 1: Photos illustrating the field sampling steps. (a) Multipoint sampling; (b) wrap and seal; (c) mark ore sample.

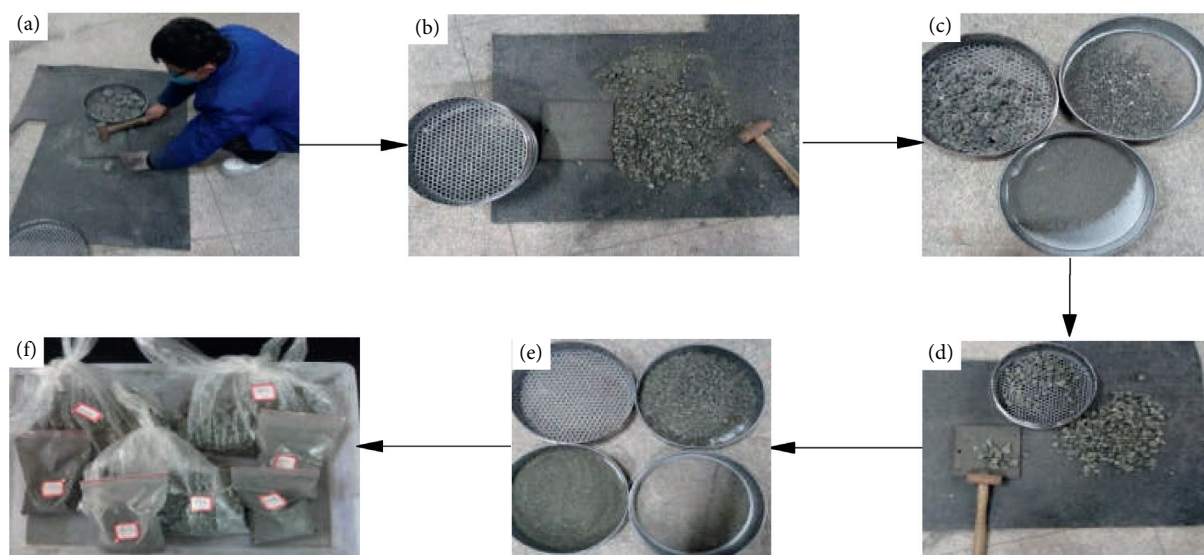


FIGURE 2: Coarse crushing process of ore samples.

**2.2. Experimental Methods.** Explosion pressure and MEC are important parameters to characterize the severity of dust explosion consequences. The explosion characteristic parameters of the metal sulfide dust ore clouds were investigated using a 20 L explosion sphere vessel (TD-20L DG, Safety Engineering Research Center of Northeastern University, China; implementing Standards of GB/T 16425-1996, ISO 6184/1-1985, and ASTM E 1226-2005 [28–30]), which comprised a 20 L stainless steel spherical container, a 0.6 L dust container, a dust dispersion system, a pressure detection system, an automatic ignition system, a wireless data transmission system, and a data acquisition system (Figure 5). The explosion chamber was partially vacuumed to 0.04 MPa, and the dispersing air pressure was set to 2.1 MPa [31]. After opening the solenoid valve, the air and metal sulfide ore dust were dispersed into the explosion chamber through high-pressure gas; a chemical igniter of

10 kJ energy located in the center of the explosion chamber was ignited after a time delay of 60 ms. Furthermore, the explosion pressure of metal sulfide ore dust was recorded using a pressure sensor, and the trend of the explosion pressure over time was recorded using a data acquisition system.

**2.2.1. Preparation of Ignition Head.** The explosion sphere vessel usually uses a chemical ignition head as the detonating source [32], but electric sparks are generated by a discharge device as the detonating source. Among them, the explosion pressure of the chemical ignition head is unstable, which needs to be checked before use. A high-frequency interference exists in the electric spark discharge, which needs to be filtered, and the high energy electric spark ignition circuit needs to be improved [33]. Through comprehensive



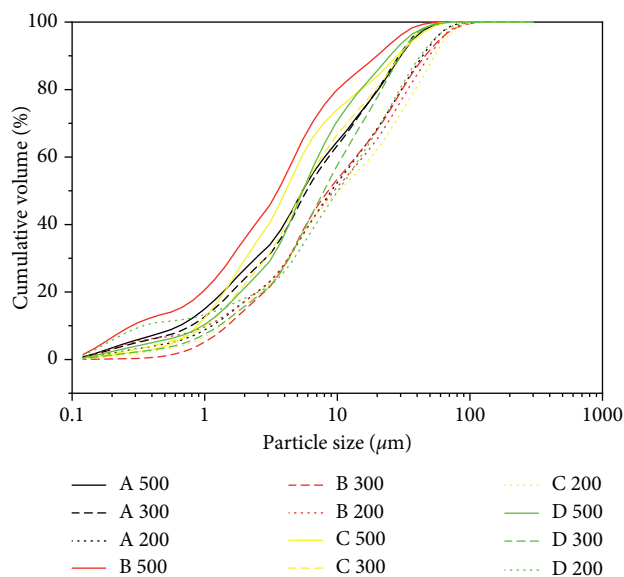
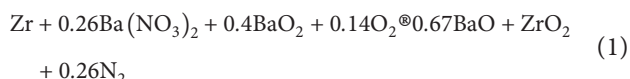


FIGURE 3: The particle size analysis curves of ore samples.

comparison, we used the checked chemical ignition head as the detonating source in this study, and the fabrication method used was as per the ISO-6184/1-1985 standard [29].

Barium nitrate and barium dioxide were ground and passed through a 200 mesh using a mortar and screened and dried in a thermostatic box. Zirconium powder was flammable, so the zirconium powder stored in water was placed in a constant temperature box. The zirconium powder was dried at 105°C until it evaporated, and then, the temperature was adjusted to 80°C to dry the caked zirconium powder into powder. After mixing the zirconium powder, barium nitrate and barium peroxide in the proportion of 4:3:3 (referring to equation (1)), weighing 2.4 g and being wrapped with around a lead wire, were used to produce an ignition head of 10 kJ (as presented in Figure 6). Five of the ignition heads with the same ignition energy were randomly selected for the blank test (only ignition head, without dust injection). The measured explosion pressures of the ignition head are 0.1, 0.11, 0.11, 0.12, and 0.12 MPa, which are all in the range of  $0.11 \pm 0.01$  MPa, and the ignition head meets the requirements of a 10 kJ ignition energy in GB/T 16425-1996 [28]. Similarly, the ignition heads of 1 kJ, 2 kJ, 3 kJ, 4 kJ, 6 kJ, 8 kJ, 9 kJ, and 12 kJ were made for test, one ignition head under each energy was randomly selected for blank experiment, and the characteristics of ignition head explosion with different energy are shown in Table 3.



**2.2.2. Test on Explosion Pressure of Metal Sulfide Ore Dust Clouds.** The MEC of common dust is mainly concentrated in the range from 20 to 60 g/m<sup>3</sup>, and the upper explosive limit is concentrated in the range of 2000 to 6000 g/m<sup>3</sup>. Combined with the explosive limit range of common dust and referring to GB/T 16426-1996 [34], six basic

concentrations (60, 250, 500, 750, 1000, and 1500 g/m<sup>3</sup>) were set as the reference points of explosion pressure for the metal sulfide ore dust clouds test. The  $P_{\max}$ ,  $(dP/dt)_{\max}$ , and  $K_{st}$  of each data point were obtained by the test. The explosibility of the metal sulfide ore dust can be judged by analyzing these three explosion pressure parameters of each base point. If the above concentration range is explosive, the dust can explode, and the MEC test can be carried out. Otherwise, it is considered that the ignition energy of 10 kJ is insufficient to ignite the sulfide dust in the range of 1500 g/m<sup>3</sup>, and the metal sulfide ore dust is regarded as inert dust which is not explosive [35].

**2.2.3. Test on MEC of Metal Sulfide Ore Dust Clouds.** The MEC of metal sulfide ore dust clouds was analyzed for the explosive test group. By referring to GB/T 16425-1996 [28], the explosible concentration was gradually narrowed to the interval between the MEC and the maximum unexploded concentration in the explosion pressure test. First, the maximum unexploded concentration was taken as the lower limit of the interval, and the integer times of 10 g/m<sup>3</sup> were taken to increase the test sample. When the pressure value of a certain concentration ( $C_1$ ) was equal to or greater than 0.15 MPa, the dust concentration was reduced to the range of 10 g/m<sup>3</sup>. If the pressure value of a certain concentration ( $C_2$ ) was less than 0.15 MPa, repeated tests were needed until the three test results are less than 0.15 MPa, and then the MEC of this sample group was between  $C_2$  and  $C_1$ .

### 3. Results and Discussion

**3.1. Test Results of Explosion Strength of Metal Sulfide Ore Dust Clouds.** According to the experimental design, explosive pressure tests were carried out for the high sulfur group (B), medium sulfur group (C), and low sulfur group (D). Sample A500 of the ultra-high sulfur group (A) was added because the sulfur content of the ultra-high sulfur group was higher than 30%, which reached the sulfur concentration standard. The additional A500 sample was mainly used for comparative analysis. A total of 10 groups were tested. By applying the explosion pressure tests, we obtained three parameters of the explosive pressure of mineral sulfide ore dust. The experimental results are listed in Tables 4–7.

**3.1.1. Classification of Explosion Pressure of Metal Sulfide Ore Dust Clouds.** The explosion pressure of dust can be determined by the method of ISO6184/1-1985. Tables 4–7 show that the explosion index of each test group is not more than 8 MPa·m·s<sup>-1</sup>, and the  $(dP/dt)_{\max}$  is not more than 30 MPa·s<sup>-1</sup>, which obviously conforms to the standard of St1 ( $K_{st} = 0-20$  MPa·m·s<sup>-1</sup>;  $(dP/dt)_{\max} = 0-73.7$  MPa·s<sup>-1</sup>) [29]. Therefore, for metal sulfide ore dust with a sulfur content of less than 37.9%, the explosion intensity is in the St1 grade, which indicates weak explosive dust [29].

**3.1.2. Effect of Dust Cloud Concentration on  $P_{\max}$  of Metal Sulfide Ore Dust Clouds.** The fitting curve of explosive pressure for all of the metal sulfide ore dusts examined is

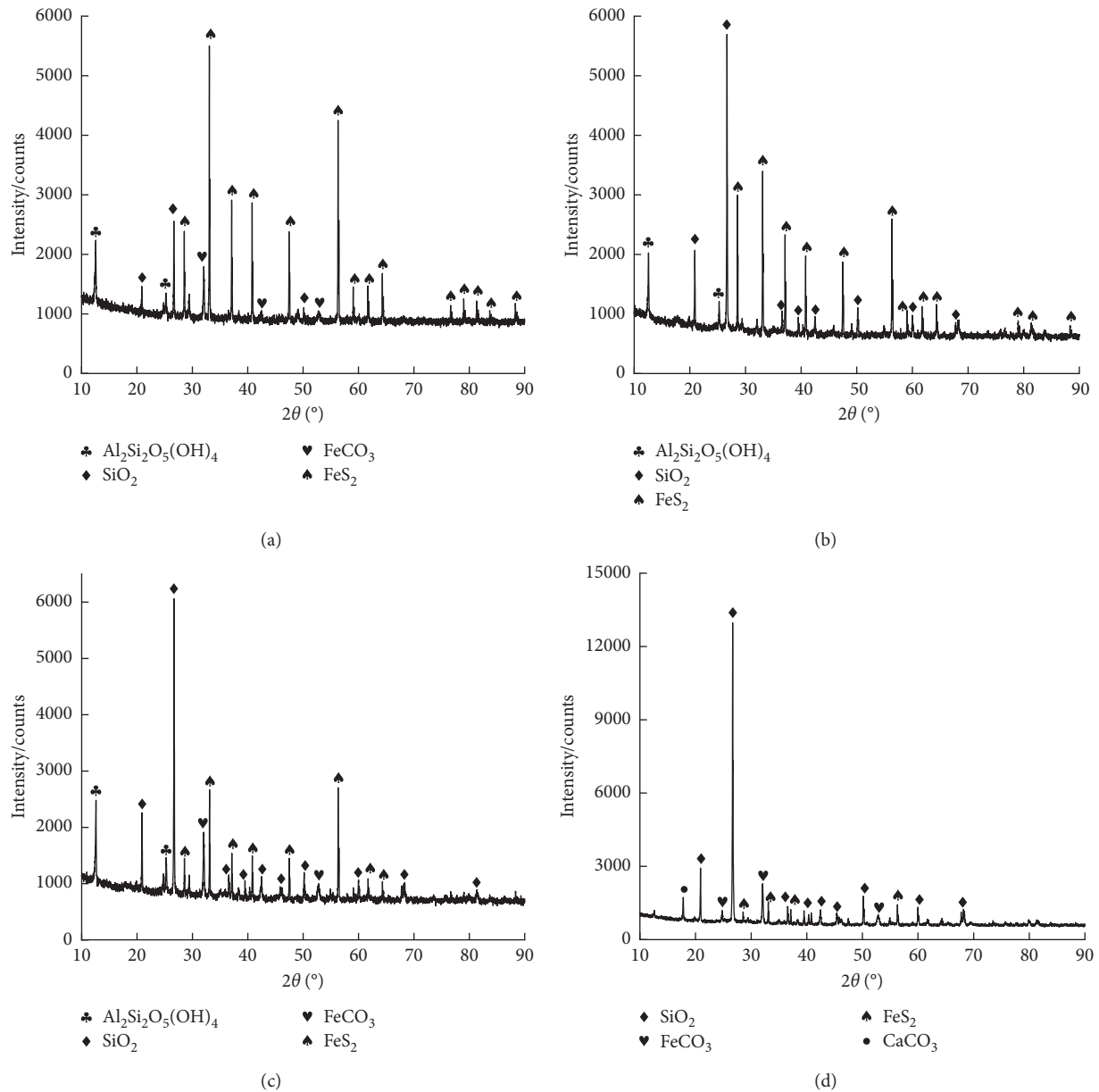


FIGURE 4: XRD spectra of four types of metal sulfide ore samples. (a) Class A ore sample; (b) Class B ore sample; (c) Class C ore sample; (d) Class D ore sample.

TABLE 2: Elemental composition of four types of metal sulfide ore dusts.

| Sample type | Fe    | S     | Si    | Al   | Cu   | Mn   | Zn   | Ti   | Ca   | K    | Other elements |
|-------------|-------|-------|-------|------|------|------|------|------|------|------|----------------|
| A           | 38.71 | 34.33 | 3.75  | 1.67 | 0.88 | 0.50 | 0.32 | 0.04 | 0.07 | 0.03 | 19.70          |
| B           | 35.90 | 26.95 | 4.55  | 1.46 | 1.06 | 0.39 | 0.15 | 0.05 | 0.09 | 0.00 | 29.40          |
| C           | 24.07 | 19.58 | 16.82 | 6.10 | 0.44 | 0.13 | 0.03 | 0.10 | 0.09 | 1.11 | 31.53          |
| D           | 20.43 | 7.65  | 12.02 | 4.05 | 0.47 | 0.82 | 0.06 | 0.10 | 0.14 | 0.87 | 53.39          |

summarized in Figure 7. In the A500 group, even at a lower concentration range of  $60 \text{ g/m}^3$ ,  $P_{\max}$  reached 0.16 MPa, and, at a higher concentration range of  $1500 \text{ g/m}^3$ , did not peak either, indicating that the metal sulfide ore dust in this group readily explodes as compared with that in the other groups. In the A500, B200, B300, B500, and C200 groups, the

analysis and fitting curves show that the  $P_{\max}$  of sulfide dust increases rapidly in the range of  $60\text{--}500 \text{ g/m}^3$ , but after the concentration exceeds  $500 \text{ g/m}^3$ , the rising trend of  $P_{\max}$  is relatively smoother. Even when the concentration reaches  $1500 \text{ g/m}^3$ , the explosion pressure does not reach the peak value, and the corresponding explosion pressure is

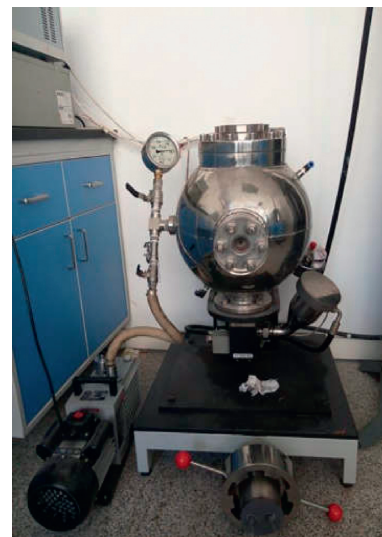
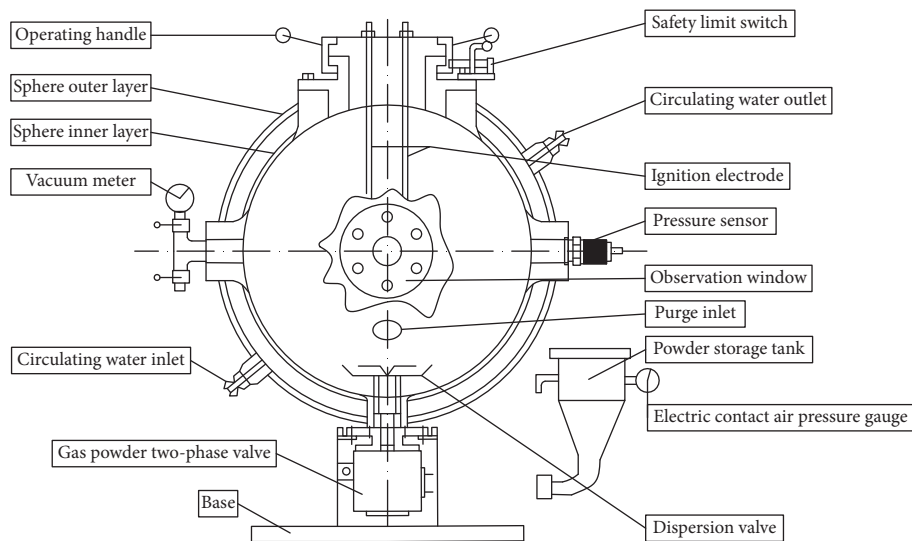


FIGURE 5: 20 L explosion sphere vessel schematic diagram and physical diagram.



(a)



(b)



(c)

FIGURE 6: Fabrication of ignition heads: (a) powder charge; (b) shear cut; (c) end product.

TABLE 3: Characteristics of ignition head explosion with different energy.

| Ignition head energy (kJ) | Ignition head powder quantity (g) | $P_{\max}$ (MPa) | $(dP/dt)_{\max}$ (MPa·s <sup>-1</sup> ) | $K_{st}$ (MPa·m·s <sup>-1</sup> ) |
|---------------------------|-----------------------------------|------------------|---|-----------------------------------|
| 1                         | 0.24                              | 0.013            | 5.20                                    | 1.41                              |
| 2                         | 0.48                              | 0.031            | 7.09                                    | 1.92                              |
| 3                         | 0.72                              | 0.046            | 5.67                                    | 1.54                              |
| 4                         | 0.96                              | 0.050            | 6.61                                    | 1.80                              |
| 6                         | 1.44                              | 0.069            | 6.14                                    | 1.67                              |
| 8                         | 1.92                              | 0.090            | 9.92                                    | 2.69                              |
| 9                         | 2.16                              | 0.095            | 8.97                                    | 2.44                              |
| 10                        | 2.40                              | 0.120            | 8.03                                    | 2.18                              |
| 12                        | 2.88                              | 0.130            | 13.23                                   | 3.59                              |

0.33 MPa, the sulfur content of group A 500 exceeds 30%, and its properties belong to the sulfur concentrate. The  $P_{\max}$  values of B200, B300, B500, and C200 groups increase first and then decrease with increasing concentration. This is because when the concentration is low, the air in the 20 L

explosion sphere vessel is sufficient, and the dust clouds formed do not reach the saturated concentration; therefore, with increasing concentration, the  $P_{\max}$  also increases [36]. When the suspended dust clouds tend to become saturated, there exists an optimum concentration to make the  $P_{\max}$

TABLE 4: Summary of explosion pressure data for A group.

| Sample type | Sulfur content (%) | D50 ( $\mu\text{m}$ ) | Concentration ( $\text{g}\cdot\text{m}^{-3}$ ) | $P_{\text{max}}$ (MPa) | $(dP/dt)_{\text{max}}$ ( $\text{MPa}\cdot\text{s}^{-1}$ ) | $K_{\text{st}}$ ( $\text{MPa}\cdot\text{m}\cdot\text{s}^{-1}$ ) | Whether or not to explode |
|-------------|--------------------|-----------------------|--|------------------------|---|---|---------------------------|
| A500-1      | 37.90              | 4.829                 | 60   | 0.16                   | 15.59   | 4.23  | Yes                       |
| A500-2      |                    |                       | 250  | 0.22                   | 18.89   | 5.13  | Yes                       |
| A500-3      |                    |                       | 500  | 0.29                   | 15.12   | 4.10  | Yes                       |
| A500-4      |                    |                       | 750  | 0.29                   | 17.48   | 4.74  | Yes                       |
| A500-5      |                    |                       | 1000   | 0.30                   | 27.87   | 7.56  | Yes                       |
| A500-6      |                    |                       | 1500   | 0.33                   | 19.37   | 5.26  | Yes                       |

TABLE 5: Summary of explosion pressure data for B group.

| Sample type | Sulfur content (%) | D50 ( $\mu\text{m}$ ) | Concentration ( $\text{g}\cdot\text{m}^{-3}$ ) | $P_{\text{max}}$ (MPa) | $(dP/dt)_{\text{max}}$ ( $\text{MPa}\cdot\text{s}^{-1}$ ) | $K_{\text{st}}$ ( $\text{MPa}\cdot\text{m}\cdot\text{s}^{-1}$ ) | Whether or not to explode |
|-------------|--------------------|-----------------------|--|------------------------|---|---|---------------------------|
| B200-1      | 25.68              | 9.467                 | 60   | 0.14                   | 16.06   | 4.36  | No                        |
| B200-2      |                    |                       | 250  | 0.15                   | 28.34   | 7.69  | Yes                       |
| B200-3      |                    |                       | 500  | 0.18                   | 14.64   | 3.97  | Yes                       |
| B200-4      |                    |                       | 750  | 0.19                   | 15.59   | 4.32  | Yes                       |
| B200-5      |                    |                       | 1000   | 0.25                   | 12.28   | 3.33  | Yes                       |
| B200-6      |                    |                       | 1500   | 0.19                   | 25.03   | 6.80  | Yes                       |
| B300-1      | 26.18              | 6.185                 | 60   | 0.11                   | 8.03  | 2.18  | No                        |
| B300-2      |                    |                       | 250  | 0.15                   | 16.06   | 4.36  | Yes                       |
| B300-3      |                    |                       | 500  | 0.16                   | 14.17   | 3.85  | Yes                       |
| B300-4      |                    |                       | 750  | 0.19                   | 12.28   | 3.33  | Yes                       |
| B300-5      |                    |                       | 1000   | 0.24                   | 14.64   | 3.97  | Yes                       |
| B300-6      |                    |                       | 1500   | 0.22                   | 16.06   | 4.36  | Yes                       |
| B500-1      | 25.60              | 3.563                 | 60   | 0.11                   | 7.09  | 1.29  | No                        |
| B500-2      |                    |                       | 250  | 0.15                   | 20.31   | 5.51  | Yes                       |
| B500-3      |                    |                       | 500  | 0.19                   | 25.51   | 6.92  | Yes                       |
| B500-4      |                    |                       | 750  | 0.20                   | 25.03   | 6.80  | Yes                       |
| B500-5      |                    |                       | 1000   | 0.21                   | 11.81   | 3.21  | Yes                       |
| B500-6      |                    |                       | 1500   | 0.18                   | 13.23   | 3.59  | Yes                       |

TABLE 6: Summary of explosion pressure data for C group.

| Sample type | Sulfur content (%) | D50 ( $\mu\text{m}$ ) | Concentration ( $\text{g}\cdot\text{m}^{-3}$ ) | $P_{\text{max}}$ (MPa) | $(dP/dt)_{\text{max}}$ ( $\text{MPa}\cdot\text{s}^{-1}$ ) | $K_{\text{st}}$ ( $\text{MPa}\cdot\text{m}\cdot\text{s}^{-1}$ ) | Whether or not to explode |
|-------------|--------------------|-----------------------|--|------------------------|---|---|---------------------------|
| C200-1      | 17.12              | 9.287                 | 60   | 0.13                   | 11.81   | 3.21  | No                        |
| C200-2      |                    |                       | 250  | 0.12                   | 11.81   | 3.21  | No                        |
| C200-3      |                    |                       | 500  | 0.13                   | 12.28   | 3.33  | No                        |
| C200-4      |                    |                       | 750  | 0.16                   | 12.28   | 3.33  | Yes                       |
| C200-5      |                    |                       | 1000   | 0.15                   | 12.75   | 3.46  | Yes                       |
| C200-6      |                    |                       | 1500   | 0.12                   | 13.23   | 3.59  | No                        |
| C300-1      | 15.46              | 6.098                 | 60   | 0.12                   | 11.81   | 3.21  | No                        |
| C300-2      |                    |                       | 250  | 0.12                   | 10.86   | 2.95  | No                        |
| C300-3      |                    |                       | 500  | 0.13                   | 12.28   | 3.33  | No                        |
| C300-4      |                    |                       | 750  | 0.14                   | 12.75   | 3.46  | No                        |
| C300-5      |                    |                       | 1000   | 0.12                   | 12.75   | 3.46  | No                        |
| C300-6      |                    |                       | 1500   | 0.10                   | 14.64   | 3.97  | No                        |
| C500-1      | 15.96              | 3.313                 | 60   | 0.11                   | 7.56  | 2.05  | No                        |
| C500-2      |                    |                       | 250  | 0.12                   | 11.34   | 3.08  | No                        |
| C500-3      |                    |                       | 500  | 0.13                   | 12.28   | 3.33  | No                        |
| C500-4      |                    |                       | 750  | 0.11                   | 11.81   | 3.21  | No                        |
| C500-5      |                    |                       | 1000   | 0.13                   | 12.28   | 3.33  | No                        |
| C500-6      |                    |                       | 1500   | 0.13                   | 15.59   | 4.23  | No                        |

reach its peak value. As the concentration continues to increase, the air in contact with the dust particle unit area is gradually reduced, leading to the explosion of the dust

particles and the flame propagation of the explosion, and the  $P_{\text{max}}$  is also reduced. When the concentration exceeds the upper explosion limit, the amount of air in the device is

TABLE 7: Summary of explosion pressure data for D group.

| Sample type | Sulfur content (%) | D50 ( $\mu\text{m}$ ) | Concentration ( $\text{g}\cdot\text{m}^{-3}$ ) | $P_{\max}$ (MPa) | $(dP/dt)_{\max}$ ( $\text{MPa}\cdot\text{s}^{-1}$ ) | $K_{\text{st}}$ ( $\text{MPa}\cdot\text{m}\cdot\text{s}^{-1}$ ) | Whether or not to explode |
|-------------|--------------------|-----------------------|--|------------------|---|---|---------------------------|
| D200-1      | 9.18               | 9.511                 | 60   | 0.12             | 9.45  | 2.56  | No                        |
| D200-2      |                    |                       | 250  | 0.12             | 14.17   | 3.85  | No                        |
| D200-3      |                    |                       | 500  | 0.11             | 13.23   | 3.59  | No                        |
| D200-4      |                    |                       | 750  | 0.11             | 13.23   | 3.59  | No                        |
| D200-5      |                    |                       | 1000   | 0.12             | 11.34   | 3.08  | No                        |
| D200-6      |                    |                       | 1500   | 0.098            | 15.59   | 4.23  | No                        |
| D300-1      | 9.74               | 7.158                 | 60   | 0.13             | 21.73   | 5.90  | No                        |
| D300-2      |                    |                       | 250  | 0.13             | 15.12   | 4.10  | No                        |
| D300-3      |                    |                       | 500  | 0.13             | 18.89   | 5.13  | No                        |
| D300-4      |                    |                       | 750  | 0.12             | 20.78   | 5.64  | No                        |
| D300-5      |                    |                       | 1000   | 0.13             | 19.84   | 5.39  | No                        |
| D300-6      |                    |                       | 1500   | 0.13             | 12.28   | 3.33  | No                        |
| D500-1      | 8.45               | 5.039                 | 60   | 0.12             | 10.86   | 2.95  | No                        |
| D500-2      |                    |                       | 250  | 0.10             | 19.84   | 5.39  | No                        |
| D500-3      |                    |                       | 500  | 0.12             | 26.92   | 7.31  | No                        |
| D500-4      |                    |                       | 750  | 0.13             | 19.37   | 5.26  | No                        |
| D500-5      |                    |                       | 1000   | 0.13             | 25.98   | 7.05  | No                        |
| D500-6      |                    |                       | 1500   | 0.11             | 21.26   | 5.77  | No                        |

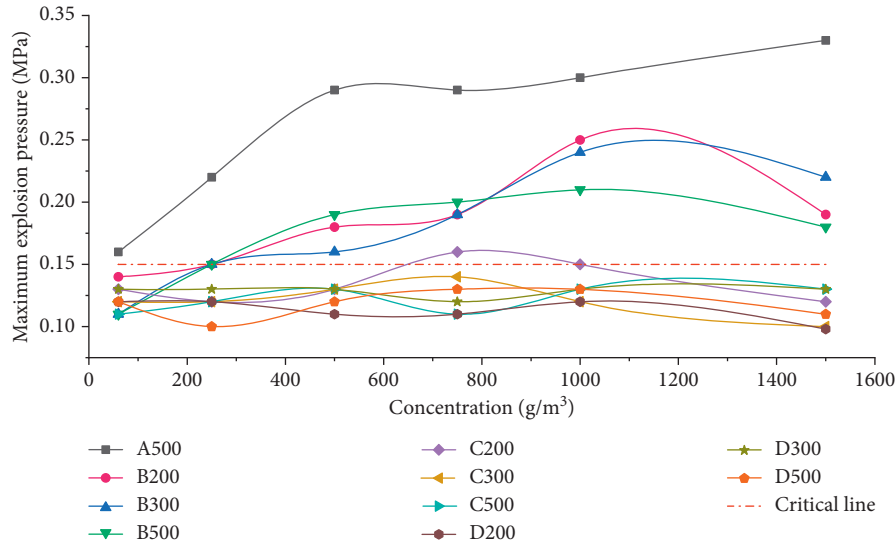


FIGURE 7: Maximum explosion pressure fitting curve of the explosive test group.

insufficient, the dust particles can only be ignited or deflagrated in a small range, and the flame conduction of the explosion is blocked, and the dust is nonexplosive.

The  $P_{\max}$  values of the C300, C500, D200, D300, and D500 groups were less than 0.15 MPa, and the fitting curve was below the critical line (critical line is the  $P_{\max} = 0.15$  MPa line). When the ignition energy is 10 kJ and the  $P_{\max}$  of dust  $\geq 0.15$  MPa, it is considered that the dust was explosive, as shown in [28]. MATLAB was used to fit the above data of the A500, B200, B300, B500, and C200 groups to the fourth-degree polynomial, and the corresponding fitting curve equation and correlation coefficient were obtained. The equations are given in formulas (2)–(6). The correlation coefficient is high. We can thus use them to calculate the explosion concentration range, which was 151–1554  $\text{g}/\text{m}^3$ ,

264–1588  $\text{g}/\text{m}^3$ , 239–1676  $\text{g}/\text{m}^3$ , and 659–1029  $\text{g}/\text{m}^3$  for the B200, B300, B500, and C200 groups, respectively:

$$\begin{aligned} \text{A500} \quad y = & 5.442e - 7x^4 - 8.067e - 6x^3 - 7.954e - 4x^2 \\ & + 0.02304x + 0.1316 \quad R^2 = 0.9884, \end{aligned} \quad (2)$$

$$\begin{aligned} \text{B200} \quad y = & -2.584 - 6x^4 + 1.273e - 4x^3 - 1.84e - 3x^2 \\ & + 0.0126x + 0.1254 \quad R^2 = 0.9638, \end{aligned} \quad (3)$$

$$\begin{aligned} \text{B300} \quad y = & -3.389e - 6x^4 + 1.865e - 4x^3 - 3.213e - 3x^2 \\ & + 0.02454x + 0.08521 \quad R^2 = 0.9992, \end{aligned} \quad (4)$$



$$\begin{aligned} \text{B500} \quad y = & -3.163e - 7x^4 + 2.228e - 5x^3 - 8.033e - 4x^2 \\ & + 0.01554x + 0.09178 \quad R^2 = 0.9952, \end{aligned} \quad (5)$$

$$\begin{aligned} \text{C200} \quad y = & 1.77e - 6x^4 - 1.186e - 4x^3 + 0.002453x^2 \\ & - 0.0155x + 0.1463 \quad R^2 = 0.9447. \end{aligned} \quad (6)$$

**3.1.3. Effect of Sulfur Content on  $P_{\max}$  of Metal Sulfide Ore Dust Clouds.** As shown in Tables 5–7, the  $P_{\max}$  of group B with high sulfur content ranges from 0.11 MPa to 0.25 MPa, and that of group C with a medium sulfur content ranges from 0.1 MPa to 0.16 MPa. Except for group C200 with high sulfur content, both C300 and C500 groups are nonexplosive. The  $P_{\max}$  of group D with low a sulfur content ranges from 0.098 MPa to 0.13 MPa, indicating characteristics of nonexplosive dust. Metal sulfide ore dust with sulfur content higher than 17.12% can explode under an ignition energy of 10 kJ, whereas sulfide dust with a sulfur content lower than 15.96% can not explode under an ignition energy of 10 kJ. This shows that the critical sulfur content of metal sulfide ore dust cloud explosions under an ignition energy of 10 kJ is between 16 and 17%. Thus, when the sulfur content of metal sulfide ore dust is higher than the critical sulfur content, it is classified as explosive dust, and when it is lower than the critical sulfur content, it is classified as nonexplosive dust.

The results show that the color of the metal sulfide ore dust changes from light gray to dark with increasing sulfur content before explosion. The metal sulfide ore dust after explosion is red and becomes darker with increasing sulfur content. As shown in Table 2, through elemental analysis of the metal sulfide ore dust before explosion, we found that the proportion of Fe elements in the metal sulfide ore dust is largest and that an increase in the sulfur content in all test groups resulted in a greater proportion of Fe elements. Therefore, the main participants in the explosion are the sulfur compounds in the metal sulfide ore dust. Because  $\text{Fe}^{2+}$  in the sulfur compounds in the metal sulfide ore dust is oxidized during explosion, oxides of  $\text{Fe}^{3+}$  are generated, which make the powder of the metal sulfide ore dust after the explosion brown. As the content of Fe increases with increasing sulfur content, and the color of the metal sulfide ore dust after the explosion becomes more red. To verify this experimental phenomenon, we characterized the explosion product. The characterization results are shown in Figure 8.  $\text{Fe}_2\text{O}_3$  was present in the product, which is consistent with the analysis results.

**3.2. Test Results of the MEC of Metal Sulfide Ore Dust Clouds.** The results of Tables 5–6 show that the B200, B300, B500, and C200 groups can explode at a certain dust concentration. Therefore, the above four groups were tested, and the MECs were obtained. The results provide a basis for controlling sulfide dust concentration and preventing sulfide

dust explosion in mines with high sulfur concentrations. The results of the tests are shown in Table 8.

**3.2.1. Classification of Explosion Sensitivity of Metal Sulfide Ore Dust Clouds.** According to the classification standard JIS Z8817:2002 of the Japanese Industrial Standards Committee [37], the dust explosion sensitivity is divided into three grades according to the MEC, as shown in Table 9.

From Table 8, the MEC of the metal sulfide ore dust with sulfur contents less than 26.18% is higher than  $100 \text{ g/m}^3$ , and the explosion sensitivity is weak. It is necessary to form a higher dust cloud concentration before it can be ignited to explode. However, the explosion sensitivity of the metal sulfide ore dust is changeable. According to the A500 group test, when the sulfur content is higher than 37.9%, explosion can still occur at a base concentration of  $60 \text{ g/m}^3$ , indicating that the MEC is lower than this concentration, and the explosion sensitivity changes from weak to medium.

**3.2.2. Effect of Particle Size and Sulfur Content on the MEC of Metal Sulfide Ore Dust Clouds.** In this test, the MEC of metal sulfide ore dust clouds was mainly restricted by sulfur content and particle size. Table 8 shows that the MEC of the C300 group is  $640 \text{ g/m}^3$ , which is more than  $400 \text{ g/m}^3$  and higher than that of the high sulfur group. The lower sulfur content weakens the explosion of sulfide dust. The lower the ignition sensitivity, the higher the MEC. For the high sulfur group, the sulfur contents of the B200, B300, and B500 groups are 25.68%, 26.18%, and 25.60%, respectively. The error of the sulfur content in these groups is less than 0.5%, which can, thus, be regarded as having the same sulfur content. Although the MEC of B500 is about  $30 \text{ g/m}^3$  lower than that of B200 in the high sulfur group, the MEC is not completely decreased with decreasing particle size. However, the MEC of the B300 group with a particle size of  $6.185 \mu\text{m}$  is approximately  $150 \text{ g/m}^3$ . These results show that when the particle size is less than  $10 \mu\text{m}$ , the explosion sensitivity of sulfide dust is strongest, and the MEC is lowest when the particle size is less than  $10 \mu\text{m}$ .

The cause for these patterns is that when the particle size is high, more ore dust particles settle after powder spraying to form unstable ore dust clouds. Wang. et al. [38] hypothesized that as dust particle size decreases, its specific area increases, the total contact area with oxygen in the air increases, and the diffusion time of oxygen to the surface of the dust particles decreases, the phenomenon of insufficient combustion in dust particles due to anoxia is effectively weakened, and combustion is accelerated. Therefore, as particle size decreases, MEC also decreases. When the particle size is small enough (less than  $10 \mu\text{m}$ ), the ore dust can form stable mine dust clouds, which are, however, restricted by the powder spraying effect. The optimal particle size can form favorable dust turbulence, increasing the propagation efficiency of the explosion flame and reducing the corresponding MEC.

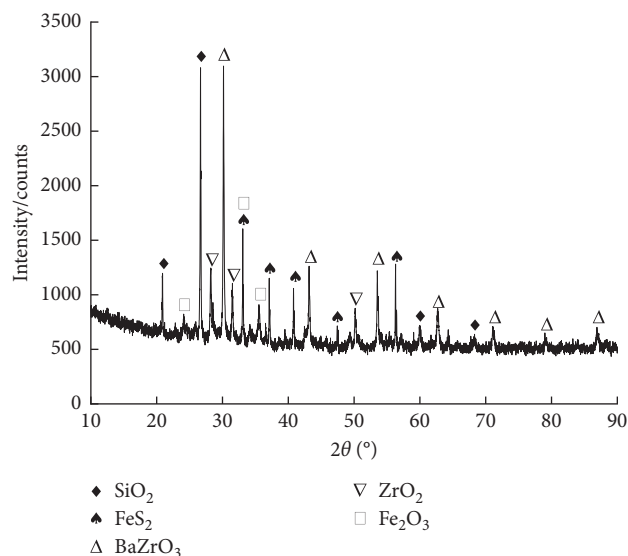


FIGURE 8: XRD spectra of the explosion product of the metal sulfide ore dust.

TABLE 8: MEC of the metal sulfide ore dust clouds.

| Sample type | Sulfur content (%) | Dust particle size D50 ( $\mu\text{m}$ ) | MEC ( $\text{g}/\text{m}^3$ ) |
|-------------|--------------------|--|-------------------------------|
| B200        | 25.68              | 9.467                                    | 230                           |
| B300        | 26.18              | 6.185                                    | 150                           |
| B500        | 25.60              | 3.563                                    | 200                           |
| C200        | 17.12              | 9.287                                    | 640                           |

TABLE 9: Classification of dust explosion sensitivity.

| $C_{\min}$ ( $\text{g}/\text{m}^3$ ) | $\geq 100$ | 45~100 | $\leq 45$ |
|--------------------------------------|------------|--------|-----------|
| Explosion sensitivity                | Weak       | Medium | Strong    |

## 4. Conclusions

The main results of the study are as follows:

- (1) By analyzing the  $(dP/dt)_{\max}$  and  $K_{st}$  of metal sulfide ore dust clouds, we classified the explosive intensity of metal sulfide ore dust clouds. The results show that metal sulfide ore dust clouds are of St1 grade and weak explosive dusts.
- (2) With increasing concentration, the  $P_{\max}$  of the explosive test group increased at first and then decreased, whereas the  $P_{\max}$  of the unexploded test group showed a discrete distribution, and no obvious trend was noted.
- (3) The critical sulfur content for explosion in the metal sulfide ore dust clouds under 10 kJ ignition energy is approximately 16–17%. Metal sulfide ore dust with a sulfur content higher than the critical one is explosive dust, and metal sulfide ore dust with a lower sulfur content than the critical one is nonexplosive dust. The analysis results show that the explosion of the ultra-high sulfur group is strongest. Explosion may occur in the middle sulfur group, and no explosion will occur in the low sulfur group, indicating that the low sulfur group is inertial dust.
- (4) The explosion sensitivity of metal sulfide ore dust is proportional to the sulfur content. The higher the sulfur content, the stronger the explosion sensitivity.
- (5) The MEC of the metal sulfide ore dust is inversely proportional to the sulfur content, i.e., the higher the sulfur content, the lower the MEC. When the particle size is less than  $10 \mu\text{m}$  (the optimum particle size is approximately  $6.185 \mu\text{m}$ ), the corresponding MEC is lowest at approximately  $150 \text{ g}/\text{m}^3$ . As particle size decreases, MEC also decreases.
- (6) The results are valuable for the prevention and control of metal sulfide ore dust explosions. However, explosion dynamics and thermodynamics are not analyzed. We will overcome these limitations in future studies.

## Data Availability

The data used to support the findings of this study are included within the article.

## Conflicts of Interest

The authors declare that they have no conflicts of interest.

## Acknowledgments

This work was sponsored by the National Natural Science Foundation of China (51874149 and 51364010). The authors are also thankful to the Associate Professor Sheng-nan Ou, University of Science and Technology Beijing for assistance with 20 L explosion sphere vessel analysis.

## References

- [1] D. K. Nordstrom, *Sulfide Mineral Oxidation*, Geological Survey, Boulder, Co, USA, 2011.
- [2] R. Walker, A. D. Steele, and D. T. B. Morgan, "Pyrophoric nature of iron sulfides," *Industrial & Engineering Chemistry Research*, vol. 35, no. 5, pp. 1747–1752, 1996.
- [3] X. Sun, Y. Z. Rao, C. Li, and S. Ma, "Test study on minimum ignition temperature of sulfide ore dust cloud," *Metal Mine*, vol. 6, pp. 175–179, 2017.
- [4] T. Chen, Q. Zhang, J. Wang, L. Liu, and S. Zhang, "Flame propagation and dust transient movement in a dust cloud explosion process," *Journal of Loss Prevention in the Process Industries*, vol. 49, pp. 572–581, 2017.
- [5] E. Danzi and L. Marmo, "Dust explosion risk in metal workings," *Journal of Loss Prevention in the Process Industries*, vol. 61, pp. 195–205, 2019.
- [6] S. Azam and D. P. Mishra, "Effects of particle size, dust concentration and dust-dispersion-air pressure on rock dust inertant requirement for coal dust explosion suppression in underground coal mines," *Process Safety and Environmental Protection*, vol. 126, pp. 35–43, 2019.
- [7] Y. Z. Rao, *Studies on Mechanism and Control Technology of Sulphide Dust Explosion*, Central South University, Changsha, China, 2018.
- [8] R. Soundararajan and P. R. Amyotte, "Explosibility hazard of iron sulphide dusts as a function of particle size," *Journal of Hazardous Materials*, vol. 51, no. 1–3, pp. 225–239, 1996.
- [9] A. H. Liu, J. Y. Chen, and X. F. Huang, "Explosion parameters and combustion kinetics of biomass dust," *Bioresource Technology*, vol. 294, Article ID 122168, 2019.
- [10] Q. Liu and P. D. Katsabanis, "Hazard evaluation of sulphide dust explosions," *Journal of Hazardous Materials*, vol. 33, no. 1, pp. 35–49, 1993.
- [11] Y. Q. Yu and J. C. Fan, "Research on explosion characteristics of sulfur dust and risk control of the explosion," *Procedia Engineering*, vol. 84, pp. 449–459, 2014.
- [12] J. Yuan, W. Huang, B. Du, N. Kuai, Z. Li, and J. Tan, "An extensive discussion on experimental test of dust minimum explosible concentration," *Procedia Engineering*, vol. 43, pp. 343–347, 2012.
- [13] J. Q. Fan, J. P. Bai, Y. S. Zhao, W. C. Yuan, Y. L. Wang, and F. Xiang, "Experimental study of factors influencing explosion characteristics of sulfur dust," *China Safety Science Journal*, vol. 28, no. 2, pp. 81–86, 2018.
- [14] Y. R. He, S. B. Zhu, M. X. Li, Q. Q. Wu, Y. Cao, and Z. Zhou, "Experimental study and numerical simulation of effect of coal particle size on dust cloud explosion," *China Safety Science Journal*, vol. 27, no. 1, pp. 53–58, 2017.
- [15] P. Bagaria, S. Prasad, J. Z. Sun, R. Bellair, and C. Mashuga, "Effect of particle morphology on dust minimum ignition energy," *Powder Technology*, vol. 355, pp. 1–6, 2019.
- [16] Q. Li, B. Lin, W. Li, C. Zhai, and C. Zhu, "Explosion characteristics of nano-aluminum powder-air mixtures in 20L spherical vessels," *Powder Technology*, vol. 212, no. 2, pp. 303–309, 2011.
- [17] J. Zhang, P. Xu, L. Sun, W. Zhang, and J. Jin, "Factors influencing and a statistical method for describing dust explosion parameters: a review," *Journal of Loss Prevention in the Process Industries*, vol. 56, pp. 386–401, 2018.
- [18] M. Mittal, "Explosion characteristics of micron- and nano-size magnesium powders," *Journal of Loss Prevention in the Process Industries*, vol. 27, no. 1, pp. 55–64, 2014.
- [19] Y. Z. Rao, Z. J. Liu, X. M. Hong, M. S. Yang, and B. Chen, "Effect of sulfur content on minimum ignition energy of sulfide dust clouds," *Metal Mine*, vol. 47, no. 4, pp. 173–177, 2018.
- [20] H. L. Shang, F. C. Yang, R. M. Xiang et al., "Influence of particle size polydispersity on coal dust explosibility," *Journal of Loss Prevention in the Process Industries*, vol. 56, pp. 444–450, 2018.
- [21] X. X. Ma, Y. Yu, Q. W. Zhang, Y. H. Li, and F. F. Liu, "Experimental study on the impact of the concentration on the explosion characteristic features of rubber," *Journal of Safety and Environment*, vol. 17, no. 4, pp. 1313–1316, 2017.
- [22] Y. S. Zhao, J. Q. Fan, J. P. Bai, C. Zeng, and Y. Wang, "Influence of dust concentration on flow field characteristics of sulfur dust during dispersion process in 20L spherical tank," *Journal of Safety Science and Technology*, vol. 14, no. 7, pp. 48–52, 2018.
- [23] C. C. Wu, *The Theoretical Basis and Application of the Combustion and Explosion*, Chemical Industry Press, Beijing, China, 2016.
- [24] H. Liu, C. Wu, F. Q. Yang, W. Pan, and M. Li, "Detection of spontaneous combustion of sulfide ores with infrared thermal imaging method," *Journal of Central South University (Science and Technology)*, vol. 42, no. 3, pp. 1425–1430, 2011.
- [25] GB/T 2462, China Standards, *Pyrites and Concentrate Neutralization Method*, State Bureau of Technical Supervision, Beijing, China, 1992.
- [26] GB/T 6003.1, China Standards, *Test Sieves—Technical Requirements and Testing—Part 1: Test Sieves of Metal Wire Cloth*, Standardization Administration of China, Beijing, China, 2012.
- [27] R. Soundararajan, *Characterization of the Dust Explosibility of the Iron Sulphides: FeS and FeS<sub>2</sub>*, Ph.D. thesis, Technical University of Nova Scotia, Halifax, Canada, 1995.
- [28] GB/T 16425, China Standards, *Determination for Minimum Explosive Concentration of Dust Clouds*, State Bureau of Technical Supervision, Beijing, China, 1996.
- [29] IX-ISO ISO: 6184/1, *Explosion Protection Systems-Part 1: Determination of Explosion Indices of Combustible Dusts in Air*, International Organization for Standardization, Switzerland, 1985.
- [30] ASTM E 1226, USA Standards, *Test Method for Pressure and Rate of Pressure Rise for Combustible Dusts*, American Society for Testing and Materials, West Conshohocken, PA, USA, 2005.
- [31] Q. Li, K. Wang, Y. Zheng, X. Mei, and B. Lin, "Explosion severity of micro-sized aluminum dust and its flame propagation properties in 20 L spherical vessel," *Powder Technology*, vol. 301, pp. 1299–1308, 2016.
- [32] R. Cui and W. Y. Cheng, "Influence of ignition energy on explosion behavior of pulverized coal," *Safety in Coal Mines*, vol. 4, no. 4, pp. 16–19, 2017.

- [33] C. L. Ren, *Experimental Investigation and Numerical Simulation of Minimum Ignition Energy of Dust Cloud*, Northeastern University, Shenyang, China, 2011.
- [34] GB/T 16426, China Standards, *Determination for Maximum Explosion Pressure and Maximum Rate of Pressure Rise of Dust Clouds*, 1996.
- [35] Q. Z. Li, C. Zhai, H. J. Wu, B. Q. Lin, and C. J. Zhu, "Investigation on coal dust explosion characteristics using 20L explosion sphere vessels," *Journal of China Coal Society*, vol. 36, no. Supp. 1, pp. 119–124, 2011.
- [36] D. Wu, W. Ferens, and K. M. Czajka, "Explosion study on the minimum ignition temperature of coal dust clouds in oxygen-fuel combustion atmospheres," *Journal of Hazardous Materials*, vol. 84, pp. 330–339, 2014.
- [37] JIS Z 8817, Japanese Standards, *Test Method for Minimum Explosible Concentration of Combustible Dusts*, Japanese Industrial Standards Committee, Tokyo, Japan, 2002.
- [38] L. Y. Wang, R. Q. Lyu, and H. B. Deng, "Study on characteristics of explosion and explosion suppression for magnesium–aluminum alloy dust with different particle size," *Journal of Safety Science and Technology*, vol. 13, no. 1, pp. 34–38, 2017.